Biochemical Pharmacology, Vol. 34, No. 24, pp. 4203–4213, 1985.
Printed in Great Britain.

0006-2952/85 $3.00 + 0.00
© 1985 Pergamon Press Ltd.

INTERACTIONS OF ANTITUMOR AGENTS AMETANTRONE* AND MITOXANTRONE (NOVATRONE)† WITH DOUBLE-STRANDED DNA

JAN KAPUSCINSKI‡ and ZBIGNIEW DARZYNKIEWICZ
Memorial Sloan-Kettering Cancer Center, New York, NY 10021, U.S.A.

(*Received* 15 *February* 1985; *accepted* 25 *April* 1985)

Abstract—Interactions of Mitoxantrone and Ametantrone with natural and synthetic nucleic acids in aqueous medium [0.15 NaCl, 5 mM 4-(2-hydroxyethyl)-1-piperazine-ethanesulfonic acid (Hepes), pH 7.0, 25°] have been studied using computer-aided spectrophotometric techniques. Absorption spectra of the drugs in monomeric and dimeric form and their complexes with DNAs at low drug/phosphate ratios (D/P) have been established. The latter were red-shifted and had lower amplitude as compared with the spectra of the free ligand's monomer; the change is consistent with the already well-established intercalative mode of drug–nucleic acid interaction. Drug–DNA equilibria have been studied using the McGhee–von Hippel model of noncooperative ligand–polymer interaction, with the correction for dimerization of drugs. Although Mitoxantrone is two orders of magnitude more potent an antitumor drug than Ametantrone, the intrinsic association constants (K_i) of both drugs were of similar magnitude. Also, no significant DNA-base specificity for either of the drugs (measured as K_i value for various homopolymers) was observed. Therefore, no correlation was apparent between the intercalative mode of binding to DNA, regardless of base composition, and the pharmacological activity of these drugs. At higher D/P ratios, a secondary mode of binding was detected by both spectroscopy and light-scattering measurement. Homopolymer-pairs and polymers containing only dI and dC were especially susceptible to this secondary type of binding. The possibility that this secondary type of binding may be responsible for the antitumor properties of the drugs is considered.

Ametantrone and its pharmacologically more active derivative, Mitoxantrone, are antitumor agents related to a series of substituted anthraquinones (for reviews see Refs. 1–4). The compounds have similar structures (Fig. 1) and are believed to bind to double-stranded (ds)§ nucleic acids by intercalation. It is unclear, however, whether or not this type of interaction is responsible for their antitumor activities, and other mechanisms have been considered (for reviews, see Refs. 2–4). Most of the evidence indicates that nucleic acids are the target of these drugs in living cells and that both DNA transcription and RNA processing are affected [5, 6].

There is a controversy regarding the base-pair specificity of these drugs [4]. Whereas no or only minimal specificity has been observed for Mitoxantrone using spectral techniques [5, 7], strong evidence for G-C preference was obtained by biochemical methods [8]. On the other hand, selective affinity towards A-T has been observed in the case of Ametantrone using a fluorochrome displacement method [7].

It has been reported recently that several intercalators including Mitoxantrone induce condensation of nucleic acids in solutions; the process appears to be preceded by destabilization of the secondary structure of nucleic acids [9, 10]. Nucleic acid condensation could distort the results of ligand–polymer interaction obtained by both spectral and dialysis techniques [11].

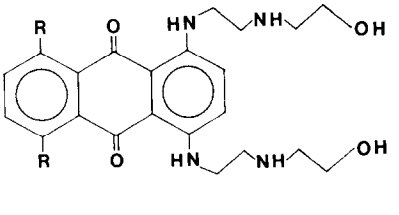

I. R=H, Ametantrone

II. R=OH, Mitoxantrone

Fig. 1. Chemical structures of Ametantrone and Mitoxantrone.

* Trade name for the salt of 1,4-bis[[2-[(2-hydroxyethyl)amino]ethyl]amino]-9,10-anthracenedione (Fig. 1, I). Abbreviations: HAQ, ANT; NSC-287513.

† Trade name for the salt of 1,4-dihydroxy-5,8-bis[[2-[(2-hydroxyethyl)amino]ethyl]amino]-9,10-anthracenedione (Fig. 1, II). Abbreviation: DHAQ; NSC-279836 and NSC-301739.

‡ Address all correspondence to: Jan Kapuscinski, Ph.D., Sloan-Kettering Institute for Cancer Research, Walker Laboratory, 145 Boston Post Road, Rye, NY 10580.

§ Abbreviations: ds, double-stranded; D/P, drug/phosphate molar ratio; r, binding density; n, binding site size; ω, cooperativity coefficient; K_I, intrinsic association constant; K_D, dimerization constant; λ, wavelength; λi, isosbestic point; MSE, mean square error; E, molar extinction coefficient; and C, molar concentration. Subscripts: M, monomer; D, dimer; T, total; F, free; B, bound; S, sample; and P, polymer.

The objective of the present study was to measure the affinity of Ametantrone and Novatrone for double-stranded nucleic acids to determine if the intercalative mode of binding correlates with their pharmacological activities. Also, by measurement of the affinity of ligands for synthetic polymers of various base composition, we hoped to clarify the problem of base specificity of these drugs. The affinity studies were done by spectrophotometric methods. Parallel light-scattering measurements were performed in these studies to assure that the ligand-induced condensation of nucleic acids did not interfere with results of the spectrophotometric assays.

MATERIALS AND METHODS

Nucleic acids

Calf thymus DNA was obtained from Sigma (St. Louis, MO); poly(dG)·poly(dC) was from Boehringer Mannheim (Indianapolis, IN); poly(dG-dC)·poly(dG-dC), poly(dA)·poly(dT), poly(dA-dT)·poly(dA-dT), poly(dI)·poly(dC) and poly(dI-dC)·poly(dI-dC) were from P. L. Biochemicals (Milwaukee, WI). The concentration of nucleic acids was determined by u.v. absorption using molar extinction coefficients supplied by the vendor. The double-strandedness of the polymers was confirmed by their hyperchromicity (>30%), and typical thermal denaturation transitions [measured in 0.1 M NaCl, 5 mM 4-(2-hydroxyethyl)-1-piperazine-ethanesulfonic acid (Hepes), pH 7.0; 1°/min]. The secondary structure of poly(dG)·poly(dC) was confirmed by fluorescence enhancement of ethidium bromide as described [12, 13].

Ligands

Mitoxantrone from American Cyanamid (Pearl River, NY) was provided by Dr. Z. A. Arlin of the N.Y. Medical College in Valhalla. Ametantrone was obtained through the Investigational Drug Branch, Cancer Therapy Evaluation Program, Division of Cancer Treatment, National Cancer Institute. The concentration of the ligands in buffer solutions was determined colorimetrically at the isosbestic point at $\lambda i = 682$ nm ($E_{\lambda i} = 8.36 \times 10^3\ M^{-1}\,cm^{-1}$ [5]) and at $\lambda i = 645$ nm ($E_{\lambda i} = 7.05 \times 10^3\ M^{-1}\,cm^{-1}$) for Mitoxantrone and Ametantrone respectively.

Buffers and solutions

All experiments were performed in the standard buffer containing 0.15 M NaCl, 5 mM Hepes, pH 7.0, at 25 ± 0.1°. The buffer was filtered through 0.45 μm pore Millex Millipore filters.

Instruments

A Zeiss PM6 digital spectrophotometer (wavelength accuracy ± 0.5 nm, band width 2 nm) equipped with a thermoelectric control unit and a subnanosecond SLM-4800 spectrofluorimeter equipped with a thermostatic holder (light-scatter measurements at 90° geometry at 310 nm, band width 8 nm [10]) were used. Digital data from the measurements were transferred to, and then processed by, an HP 9826 computer and drawn by an HP 7225A digital plotter.

Titration of nucleic acids with Ametantrone and Mitoxantrone

The 2-ml aliquots containing nucleic acid (50–100 μM) dissolved in buffer were placed in a quartz cuvette in the thermostatic holder of the spectrophotometer. The sample and the blank (buffer only) were treated with small volumes (5–20 μl) of the ligand stock solution (0.1–2 mM); following addition of the ligand the contents of the cuvettes were gently mixed and incubated for 10 min at 25°. This equilibration was necessary to obtain a stable reading. The absorption spectra were then measured at 1–5 nm intervals. Then the cuvettes were transferred to the fluorimeter, and light scattering at 350 nm was recorded as described [9, 10].

Calculations

The ligand dimerization constants (K_D) were calculated according to the method described by von Tscharner and Schwarz [14]:

$$K_D = \frac{C_T - C_M}{2C_M^2} \tag{1}$$

$$C_M = C_T \frac{E_S - E_D}{E_M - E_D} \tag{2}$$

where C_T is the total ligand concentration, measured colorimetrically at the isosbestic point (λi) of the ligand's monomer–dimer system; C_M is the monomer concentration; E_S, E_M and E_D are extinction coefficients of the sample, monomer and dimer (calculated per monomer unit), respectively, measured at wavelength $\lambda \neq \lambda i$. The method for calculation of E_M and E_D is given in the Results.

The intrinsic association constants (K_I) were calculated according to the McGhee–von Hippel model of ligand–polymer interaction [15], from the equation:

$$\frac{r}{C_M} = K_I(1 - nr)\left[\frac{1 - nr}{1 - (n-1)r}\right]^{n-1} \tag{3}$$

where r is the binding density expressed as an average number of bound ligands per polymer unit (base pair) and n is the binding site size expressed as the number of base pairs. The concentration of the ligand monomer (C_M) in equilibrium with the dimer and with the ligand–polymer complex can be calculated using equations:

$$C_M = [(1 + 8K_D \cdot C_F)^{\frac{1}{2}} - 1](4K_D)^{-1} \tag{4}$$

$$C_F = C_T \frac{E_B - E_S}{E_B - E_F} \tag{5}$$

where C_T is the total ligand concentration obtained from absorption measurements in the absence of the polymer (blank) at the isosbestic point (λi) and C_F is the free ligand concentration calculated from absorption measurements of the sample at λi; E_S, E_B and E_F are extinction coefficients of the sample, bound- and free-ligand at λi respectively. Equation 4 is obtained by solving Eqn (1) in which C_F replaces C_T, for C_M. The method by which E_B and E_F are estimated is given below (Results).

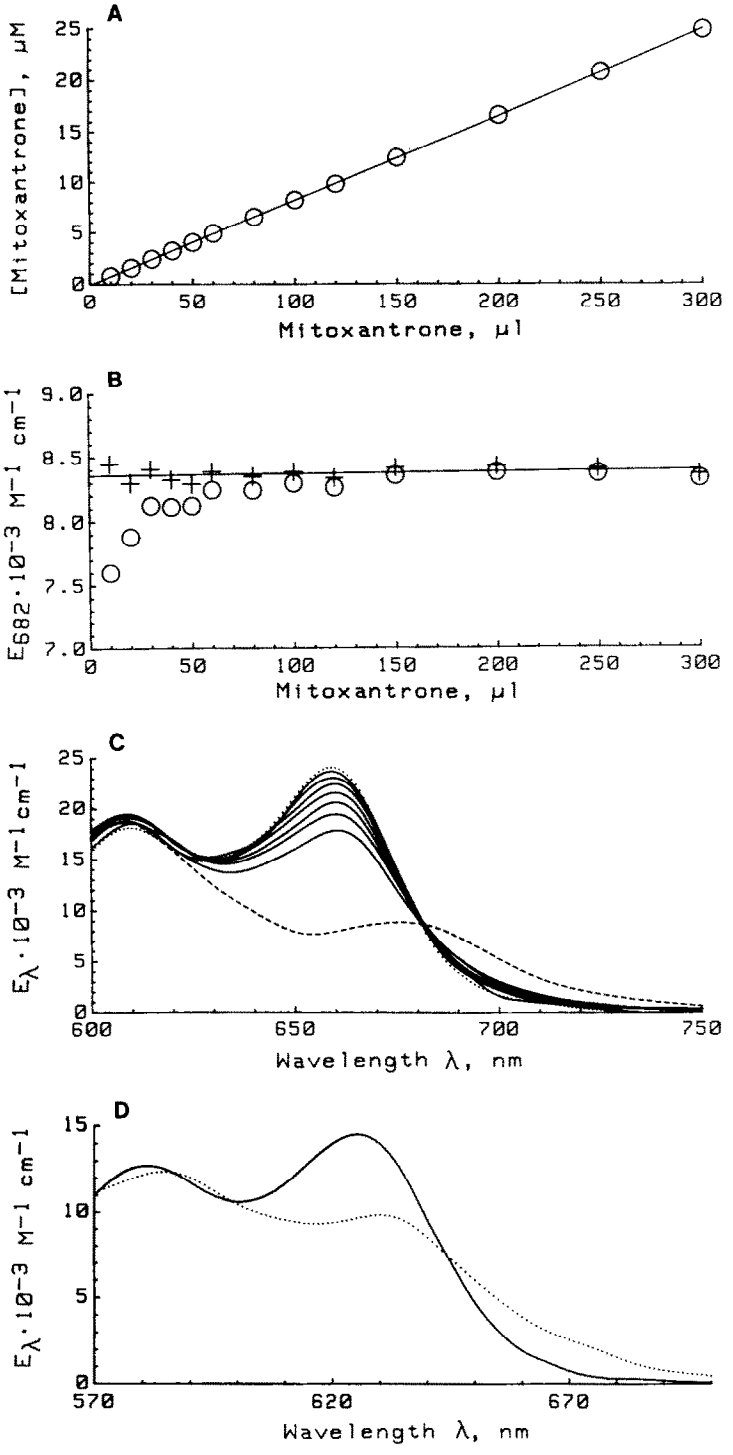

Fig. 2. (A) Properties of Mitoxantrone and Ametantrone in solution. Aliquots (2 ml) of the standard buffer were titrated with Mitoxantrone stock solution (0.166 mM). The absorption at the isosbestic point (682 nm) was measured for each point of the titration and ligand concentration, corrected for the sample volume increase, and calculated using the molar extinction coefficient $E_{682} = 8.36 \times 10^3\ M^{-1}\ cm^{-1}$. (B) Calculation of E_{682} using the results of the experiment described in (A), based on titration with the drug stock solution added to the sample (—○—), and corrected for drug absorption by the cuvette walls (5 ng/cm^2) at the first point of titration (—+—). (C) Absorption spectra of Mitoxantrone: (—) maxima from top to bottom correspond to samples of concentrations: 0.49, 0.95, 1.91, 3.77, 5.84, 9.32 and 14.02 μM respectively; (···) monomer spectrum obtained by extrapolation to zero of the square root of drug concentration; and (---) dimer spectrum calculated according to Method II. (D) Absorption spectra of Ametantrone: (—) monomer spectrum obtained by extrapolation to zero of the square root of drug concentration, and (···) dimer spectrum calculated according to Method II.

The value of r can be calculated from the known concentration of the polymer (C_p, corrected for the dilution by the added volume of ligand stock solution) according to equations:

$$r = \frac{2C_B}{C_P} \quad (6)$$

where C_B is the concentration of bound ligand:

$$C_B = C_T - C_F \quad (7)$$

With values of r and C_M estimated for several points of titrations, the K_I and n could be calculated from Eqn (3) using a computer-interactive program based on the strategy described by Wilson and Lopp [16].

RESULTS

Properties of the ligands

It has been reported that the spectrum of Mitoxantrone is concentration-dependent [5]. The precise colorimetric assay therefore can be made only at the isosbestic point (λi) at which the drug obeys the Beer–Lambert law (Fig. 2A). It has been constantly observed, however, that the values of the molar extinction coefficient $E_{\lambda i}$ calculated based on data from the very first points of titration were lower than those on the subsequent titration points (Fig. 2B). The most plausible explanation of this observation is that Mitoxantrone binds to the walls of the cuvette. This phenomenon is observed frequently for other cationic dyes, e.g. acridine orange [14]. From the shape of the titration curve it appears that Mitoxantrone binds to the quartz very strongly, but such binding is limited to relatively small quantities of the drug, which we calculated to be approximately 5 ng (11 pmoles)/cm^2 (Fig. 2B).

From the above, it is clear that an estimate of ligand concentration in the sample cannot be estimated accurately from the volume of the stock solution added to the sample but requires a colorimetric assay of the blank, as described in Materials and Methods.

Dimerization of the ligands

The dimerization constant of the ligand (K_D) can be calculated if both the extinction coefficient of the monomer (E_M) and the dimer (E_D) are known for any $\lambda \neq \lambda i$ (e.g. Ref. 14). The first coefficient was estimated by two methods:

Method I. Computer-aided extrapolation of the spectral changes to infinite dilution of the ligand, as shown for Mitoxantrone and Ametantrone (Fig. 2, C and D).

Method II. Using an interactive computer program, based on the additivity of the absorption of monomer and dimer in the mixture, it is possible to match the E_M and E_D in such a way that the mean square error (MSE) of K_D, calculated (Eqn (1) and (2)) for several samples of different ligand concentration, is minimized. More details about the method and the results of the calculation for the experiment described in the legend to Fig. 2C are presented in Table 1.

There was very good agreement between E_M values calculated by each method for both Mitoxantrone and Ametantrone (see Table 2).

Table 1 lists the composition of the samples described in the legend to Fig. 2C. The spectrum of the Mitoxantrone dimer was established from these data. Namely, calculations were made based on Eqn 2 (solved for E_D) and using the spectrum of the Mitoxantrone monomer obtained according to Method I. The results are shown in Fig. 2C. A similar procedure has been used to establish the spectra of the Ametantrone monomer and dimer (Fig. 2D, Table 2).

Spectral properties and equilibrium data of ds DNA complexes with Ametantrone

Figure 3A illustrates the changes in the visible spectrum of the drug in the presence of double-stranded DNA at various D/P ratios. The red shift of the maxima and the hypochromicity, the changes consistent with intercalative mode of binding [17], are clearly visible. Also, the quasi-isosbestic point is observed at approximately 638 nm. The spectrum of Ametantrone–calf thymus DNA has been obtained

Table 1. Dimerization of Mitoxantrone

Sample No.	Concentrations (μM) Total	Monomer	Dimer	K_D, 10^{-4} M^{-1}
1	0.490	0.478	0.006	2.734
2	0.945	0.887	0.029	3.657
3	1.910	1.726	0.092	3.093
4	3.768	3.211	0.279	2.704
5	5.837	4.642	0.598	2.773
6	9.322	6.768	1.277	2.778
7	14.020	8.852	2.584	3.298
Mean ± MSE:				3.007 ± 0.36

Dimerization constants (K_D) were calculated from the experiment described in the legend to Fig. 2C according to Equations (1) and (2). The computer-iterative program matched E_M (from 2×10^4 to 3×10^4 cm^{-1} M^{-1}; increment 100) with E_D (from 5×10^3 to 1×10^4 cm^{-1} M^{-1}; increment 100) for a minimum of MSE of seven samples. The best fit (MSE = 12%) has been obtained for $E_M = 2.41 \times 10^4$ and $E_D = 7.2 \times 10^3$ cm^{-1} M^{-1}.

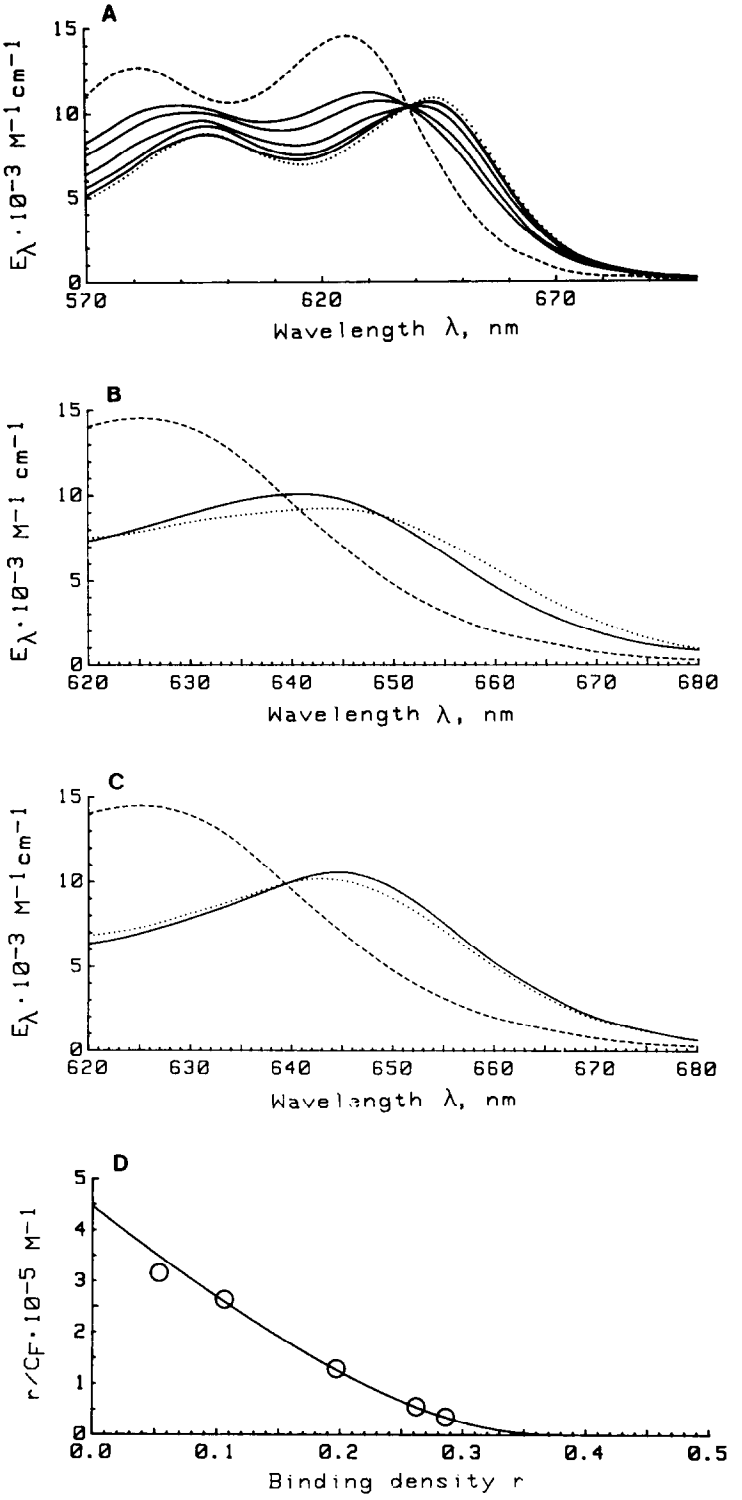

Fig. 3. (A) Absorption spectra of Ametantrone–calf thymus DNA mixtures. Key: (—) D/P ratios: 0.030, 0.060, 0.125, 0.218 and 0.301; the initial DNA concentration was 60 μM. (···) Absorption spectrum of the drug–DNA complex obtained by extrapolation to D/P equal to zero, and (---) the drug monomer. (B) Absorption spectra of Ametantrone complexes with (—) poly(dA-dT)·poly(dA-dT) and (···) poly(dA)·poly(dT) obtained from titration data by extrapolation to D/P equal to zero; (---) the drug monomer. (C) Absorption spectra of Ametantrone complexes with (—) poly(dG-dC)·poly(dG-dC) and (···) poly(dG)·poly(dC); (---) the drug monomer. (D) Scatchard plot of titration of calf thymus DNA with Ametantrone (see (A), this figure). The curve is the best fit of the McGhee–von Hippel isotherm (Eqn (3)) to the experimental points (circles) drawn by computer for $K_I = 4.46 \times 10^5\ M^{-1}$ and $n = 2.6$ base pairs. The calculations are based on the spectral data listed in Table 4.

Table 2. Spectral and dimerization data of Mitoxantrone and Ametantrone in 0.15 M NaCl, 5 mM Hepes, pH 7.0, at 25°

	λ_{max} (nm)	$E_{max}\ 10^{-3}$, $cm^{-1}M^{-1}$	E_λ, $cm^{-1}M^{-1}$ calculated according to Method I	Method II	$K_D\ 10^{-4}$, M^{-1} (± MSE)	λi (nm)	$E_{\lambda i}\ 10^{-3}$, $cm^{-1}M^{-1}$
Mitoxantrone							
Monomer	659	25.09	24.12	24.10	3.01 ± 0.36	682†	8.36†
Dimer	679	9.00*	—	7.20*			
Ametantrone							
Monomer	625	14.57	14.57	14.58	0.69 ± 0.04	645	7.05
Dimer	632	10.25*	—	9.48*			

λ_{max} and λi are the wavelengths of the last absorption maximum in the visible part of the spectrum and at an isosbestic point respectively; E_{max} and $E_{\lambda i}$ are molar extinction coefficients at these wavelengths. E_λ is the molar extinction coefficient at which the dimerization constant (K_D) was measured; λ = 660 and 625 nm for Mitoxantrone and Ametantrone respectively.

* Calculated per monomer

† From Ref. 5.

from these data by extrapolation of D/P equal to zero using a computer procedure similar to that applied to obtain a spectrum of the ligand monomer (Method I). Using the same approach, the spectra of the drug complexes with ds DNA of defined base composition and configuration have been established (Fig. 3, B and C). There are marked differences between individual spectra not only related to base-composition e.g. poly(dA)·poly(dT) vs poly(dG)·poly(dC)] but also to base-configuration [e.g. poly(dA)·poly(dT) vs poly(dA-dT)·poly(dA-dT)]. Numerical data characteristic of the visible spectra of Ametantrone–ds DNA complexes are presented in Table 3. It should be stressed that during these titrations no increase in light scattering (with respect to blank) was observed.

Quantitative studies of Ametantrone–ds DNA interactions were done based on the absorption measured at the isosbestic point of the ligand monomer–dimer system, i.e. at 645 nm. Because of the red shift, the complexes had higher extinction coefficients at this wavelength as compared to free ligand. During titrations when the D/P ratio increases, the extinction coefficient of the mixture decreases, tending asymptotically to $E_{\lambda i}$. Based on these changes in absorption, the concentrations of free and bound ligand were calculated and, after correction for the dimer concentration (as described in Materials and Methods), the results were presented on Scatchard plots (e.g. Fig. 3D). Association constants and binding site sizes of five synthetic and natural DNAs were calculated and are listed in Table 4.

Interactions of Mitoxantrone with ds DNA

At a low D/P ratio (<0.02), all DNAs listed in Table 3 when titrated with Mitoxantrone form complexes with spectral properties similar to those of Ametantrone–DNA. The data listed in Table 3 indicate a red-shift of the maxima and moderate hypochromicity as compared with the spectrum of the ligand monomer (Fig. 4). At higher D/P ratios, however, only poly(dA-dT)·poly(dA-dT), poly(dG-dC)·poly(dG-dC) and natural DNA interacted with the drug in a way which was consistent with a single-type binding site model, as was the case with Ametantrone–DNA interactions. Other polymers (Tables 3 and 4), when treated with the ligand, exhibited distinctly different spectral changes. Such changes are shown in Fig. 4B, using as an example binding to poly(dA)·poly(dT). As is evident when a specific D/P ratio threshold was achieved, a sudden drop in absorption and a blue shift of the spectra maxima of the spectra resulted. The drop in absorption was of such magnitude that some of the spectra (Fig. 4B) had lower amplitudes than those of the ligand monomer, dimer or ligand–polymer complex at low binding densities. These changes strongly suggested that at increasing ligand concentrations a second type of binding site appeared. The abrupt decrease in absorption during the titration with Mitoxantrone was paralleled by an increase in light-scattering of the samples (Fig 5). Because spectral characteristics of these light-scattering complexes are unknown and cannot be established by the present methods, the quantitative assays of free and bound ligand estimates cannot be performed.

The association constant (K_I) and binding site size (n) have been calculated for those polymers based on titration points at a very low D/P ratio in which the abnormalities, as described above, were not yet evident (Fig. 5, Table 4). However, there is a strong possibility that the secondary structural changes of the complexes (which may actually precede the light-scatter appearance and the absorption drop) can contribute to these estimates. Therefore, the data from these titrations, especially the estimate of n, should be interpreted with caution.

DISCUSSION

The data in the literature [18, 19] and our earlier [5] and present studies indicate that Mitoxantrone and Ametantrone intercalate into DNA at a low D/P ratio. Thus, both drugs increase the thermal stability of DNA [18], and their absorption spectra exhibit hypochromic and bathochromic shifts after complexing with double-stranded polymers [5]. Furthermore, Mitoxantrone, upon binding, unwinds closed circular DNA [5] and causes increase in length of the polymer molecule [19].

Studies of the interaction of Mitoxantrone and Ametantrone with biopolymers are hindered by several peculiarities of these ligands. One of the difficulties is formation of dimers and perhaps higher aggregates resulting in a multicomponent spectrum

Table 3. Spectral data of Ametantrone and Mitoxantrone complexes with ds DNAs in 0.15 M NaCl, 5 mM Hepes, pH 7.0, at 25°

	λ_{max} (nm)		$\Delta\lambda_{max}$ (nm)		$E_{max} \times 10^{-3}$, $cm^{-1}\ M^{-1}$		H%	
	Mitoxantrone	Ametantrone	Mitoxantrone	Ametantrone	Mitoxantrone	Ametantrone	Mitoxantrone	Ametantrone
Poly(dA)·poly(dT)	679	644	20	19	19.36 ± 0.12	9.27 ± 0.20	22.8	36.4
Poly(dA-dT)·poly(dA-dT)	678	641	19	16	21.91 ± 0.13	10.11 ± 0.12	12.7	30.6
Poly(dG)·poly(dC)	683	643	24	18	21.44 ± 0.10	10.20 ± 0.10	14.5	30.0
Poly(dG-dC)·poly(dG-dC)	685	645	26	20	18.51 ± 0.30	10.70 ± 0.15	26.2	26.6
Poly(dI)·poly(dC)	669		10		19.24 ± 0.30		23.3	
Poly(dI-dC)·poly(dI-dC)	681		22		22.68 ± 0.36		4.7	
Calf thymus DNA	681	644	22	19	22.54 ± 0.15	11.05 ± 0.08	10.2	24.4

λ_{max} and E_{max} are the wavelengths of the last absorption maximum in the visible part of the spectrum and the molar extinction coefficient (± mean square fitting error) at λ_{max} respectively; $\Delta\lambda_{max}$ and H% are the red shift of the maximum and percent decrease in the amplitude of the spectra as compared to the ligand monomer respectively (Table 2).

Table 4. Equilibrium data of the ligand–ds DNA complexes in 0.15 M NaCl, 5 mM Hepes, pH 7.0, at 25°

	$E_\lambda \times 10^{-3}$, $cm^{-}\ M^{-}$		n, base pairs		$K_i\ 10^{-5}$ (MSE%)	
Polymer	Mitoxantrone	Ametantrone	Mitoxantrone	Ametantrone	Mitoxantrone	Ametantrone
Poly(dA)·poly(dT)	19.10	9.25	2.9*	2.0	1.71 (22)*	2.58 (8)
Poly(dA-dT)·poly(dA-dT)	21.00	9.79	2.4	2.3	2.70 (5)	5.17 (6)
Poly(dG)·poly(dC)	21.60	10.10	7.6*	3.0	1.50 (4)*	3.43 (13)
Poly(dG-dC)·poly(dG-dC)	18.20	10.70	2.0	2.0	2.88 (9)	3.42 (9)
Poly(dI)·poly(dC)	14.70		5.0*		<2 (13)*	
Poly(dI-dC)·poly(dI-dC)	22.50		15.2*		1.16 (16)*	
Calf thymus DNA	22.50	11.00	2.6	2.6	2.52 (2)	4.46 (5)

E_λ is the molar extinction coefficient of the ligand–DNA complex at the isosbestic point of the ligand's monomer–dimer system, at $\lambda = 682$ and 645 nm for Mitoxantrone and Ametantrone respectively (see Table 2); n and K_I are the binding site size and association constant, respectively, as defined by McGee and von Hippel [15], calculated by computer as the best fit of titrations.

* The data may be affected by the secondary changes in the Mitoxantrone–DNA complex and, therefore, should be treated with caution; for explanation, see text (Discussion).

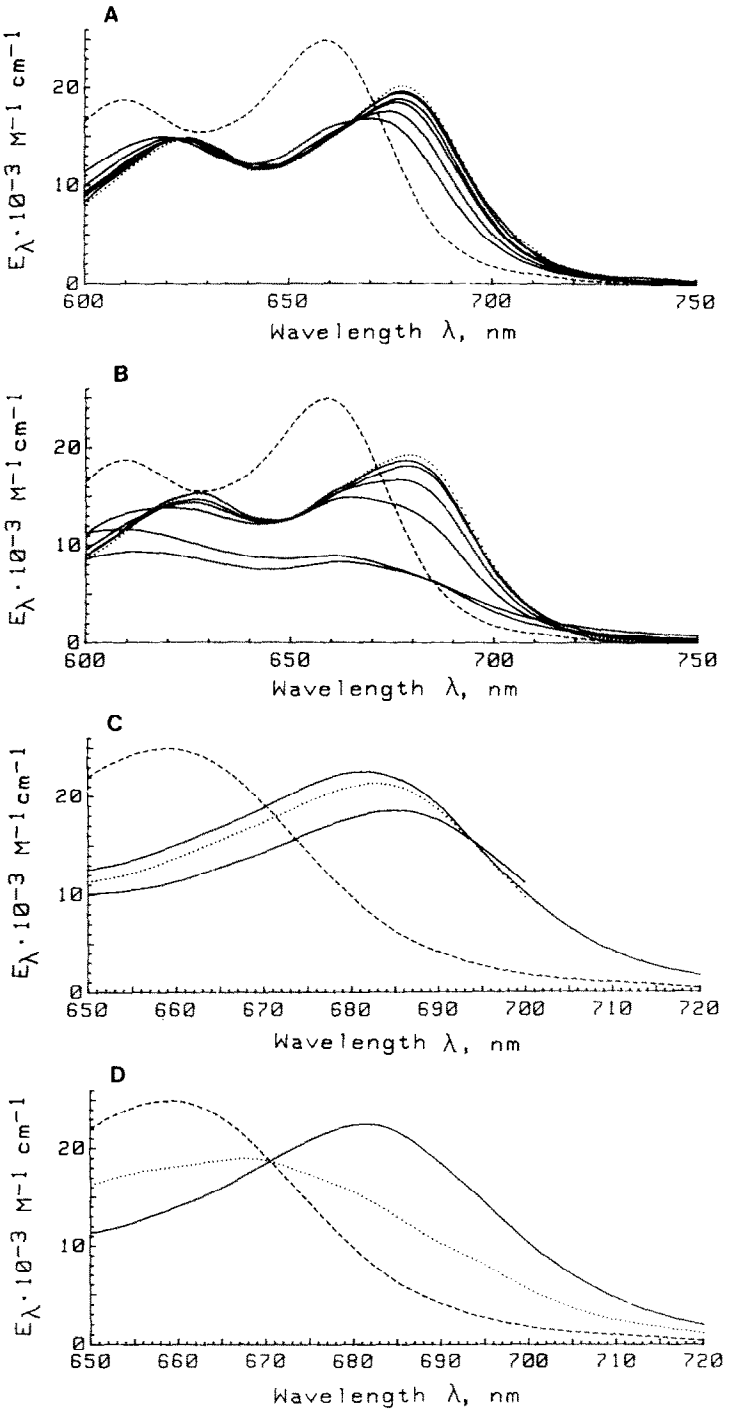

Fig. 4. (A) Titration of poly(dA-dT)·poly(dA-dT) with Mitoxantrone: (—) maxima from top to bottom represent absorption spectra of the DNA–ligand mixtures at D/P = 0.019, 0.040, 0.079, 0.123, 0.205 and 0.308 respectively; initial DNA concentration was 49 μM. (···) Spectrum of the polymer–drug complex obtained by extrapolation of the mixture spectra to D/P equal to zero, and (---) spectrum of the drug monomer. (B) Titration of poly(dA)·poly(dT) with Mitoxantrone: (—) maxima from top to bottom represent absorption spectra of the DNA–ligand mixtures at D/P: 0.018, 0.044, 0.109, 0.218, 0.325, and 0.436 respectively. The initial polymer concentration was 45 μM. (···) Spectrum of the polymer–drug complex obtained by extrapolation of the mixture spectra (initial four points of titration) to D/P equal to zero; and (---) the drug monomer. (C) Absorption spectra of Mitoxantrone with DNA obtained by extrapolation of the titration data obtained at low D/P $\leqq$0.25. Key (—) calf thymus DNA (upper curve) and poly(dG-dC)·poly(dG-dC) (lower curve); (···) poly(dG)·poly(dC); and (---) the drug monomer. (D) Absorption spectra of Mitoxantrone with DNA obtained by extrapolation of the titration data at low D/P $\leqq$0.25. Key: (—) poly(dI-dC)·poly(dI-dC); (···) poly(dI)·poly(dC); and (---) the drug monomer.

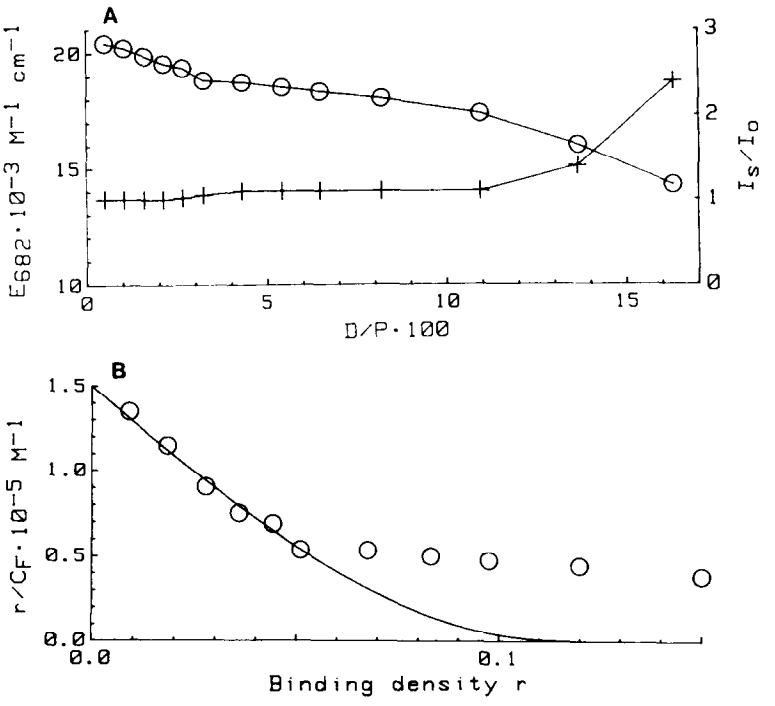

Fig. 5. Titration of poly(dG)·poly(dC) with Mitoxantrone. (A) changes in molar extinction coefficient at 682 nm (—○—, left scale) and in light scattering at 350 nm (—+—, right scale). Initial polymer concentration was 152 μM. (B) Scatchard plot of the initial eleven points of titration. The curve is the best fit of the McGhee–von Hippel isotherm (Eqn (3)) to the first six titration points (circles) drawn by computer for $K_I = 1.5 \times 10^5$ M^{-1} and $n = 7.6$ base pairs. The calculations are based on the spectral data listed in Table 4.

that is difficult to analyze (e.g. Fig. 2C). Also, ligands are absorbed by various materials, including quartz (Fig. 2B). Finally, Mitoxantrone has a tendency to condense and precipitate nucleic acids [5, 10]. In the present studies, we have tried to circumvent the above obstacles by monitoring titrations at the isosbestic point (where $E_M = E_D$, [5]), using blanks to assay the total drug concentration, and by parallel measurements of light scattering. Only those samples which showed no significant light scattering were used in calculation of the affinity data (Fig. 5).

Calculations of the intrinsic association constant (K_I) and binding site size (n) were made based on the noncooperative model of polymer–ligand interaction proposed by McGhee and von Hippel (Eqn 3, [15]). Using this approach, the value of n can be obtained consistent with the nearest-neighbor exclusion model ($n \geqq 2$ base pairs, [20]). It is possible, however, to interpret the neighbor exclusion binding as anticooperative binding (cooperative parameter $\omega \simeq 0$). The value of K_I is identical for both models; the value of n, however, calculated according to the anticooperative model is different: $m = n - 1$ ([15]; for more discussion see Ref. 21). Because, as described below, the Mitoxantrone binding site size could not be accurately measured for several synthetic polynucleotides, we have chosen for simplicity to interpret the data using the noncooperative model which describes the ligand association in the terms of two parameters (K_I and n) instead of three (K_I, m, ω).

To obtain more accurate data for the ligand binding, a correction was made to estimate the concentration of the free ligand in the monomer form. The monomer, dimer and perhaps higher aggregates* are in equilibrium in solution but only the concentration of monomer should be taken into consideration in the intercalative process as proposed by Lerman [22]. The calculation of the monomer–dimer equilibrium was made based on the method described by von Tscharner and Schwarz [14].

Because of higher accuracy in the spectral data calculations in the present study for both free and bound ligand, correction made for dimer concentration and different buffer system, the data of Mitoxantrone and its affinity to calf thymus DNA presented in Tables 3 and 4 differ somewhat from those reported in Ref. 5.

There is a significant difference between Mitoxantrone and Ametantrone in their abilities to self-association. The dimerization constant of the former is over 4-fold higher than that of the latter (Table 2). This observation can explain the differences between the spectral patterns of the DNA complexes with these ligands. Because of the low K_D of Ametantrone, the concentration of the dimer was low and, therefore, the quasi-isosbestic point at 638 nm was observed; higher dimer concentration in the case of

* No attempt has been made to estimate the concentration of aggregates higher than the dimers. It is evident from the data in Table 1 that, at the concentrations used, the proportion of higher aggregates is negligible; otherwise, the MSE of the K_D measurement would be much higher.

Mitoxantrone precluded appearance of such a point (Figs. 3A and 4A).

The spectra of both ligands complexed with DNA were red-shifted and had a lower amplitude compared with the monomer (Table 3). These effects are consistent with the intercalative mode of Mitoxantrone binding to nucleic acids [5].

The extent of the red shift and hypochromicity varied depending on the primary structure of DNAs, indicating the interaction of the drug's chromophore with different bases (Figs. 3 and 4, Table 3). The data from Table 3 also indicated that not only base composition but also different base configuration could alter the spectral properties of the intercalated ligand [e.g. poly(dI)·poly(dC) vs poly(dI-dC)·poly(dI-dC)].

The intrinsic association constants (K_I) of Ametantrone to four synthetic polymers are listed in Table 4. The lowest value was observed for poly(dA)·poly(dT), the highest for poly(dA-dT)·poly(dA-dT), i.e. 2.58×10^5 and $5.17 \times 10^5\ M^{-1}$ respectively. As expected, the value of K_I for natural DNAs had an intermediate value (Table 4). Our results agree with the findings of Roboz *et al.* [7] (who used the competitive fluorescence polarization technique) that the affinity of Ametantrone to poly(dA-dT)·poly(dA-dT) was higher than to poly(dG-dC)·poly(dG-dC) or to calf thymus DNA.

The binding site sizes (n) measured for synthetic polymers were between 2 and 3 base pairs; the value for natural polymers was again intermediate (2.6 base pairs, Table 4). The reason for non-integral values of n is unknown. It is possible, however, that a secondary mode of binding, which was observed with Mitoxantrone (and will be discussed in detail below), affected the results of experiments made at a high D/P ratio.

The results of experiments with Mitoxantrone were much more affected by this secondary process than those with Ametantrone. Despite this, the extrapolation of the data to D/P equal to zero allowed us to establish the spectra of the complexes of Mitoxantrone with several synthetic polymers and with calf thymus DNA (Figs. 3 and 4). The comparison of spectral data of these two drug complexes indicates that, in general, similar changes occur for both ligands after their binding to DNA. It should be noted, however, that the red shift ($\Delta\lambda_{max}$, Table 3) for Mitoxantrone was somewhat larger and the hypochromicity lower as compared to Ametantrone.

Based on interactions with Mitoxantrone at high D/P ratios (>0.1), the polymers in this study could be divided into two categories. The first category consisted of polymers which reacted with both Mitoxantrone and Ametantrone in a similar way, i.e. with no significant increase in light scatter for D/P up to 0.5. The Scatchard plots of these polymers indicated the presence of a single type of binding site with an n between 2.0 and 2.6 base pairs (Table 4) for binding densities up to $r \simeq 0.25$. The alternating sequences, with the exception of poly(dI-dC)·poly(dI-dC), and natural DNA belonged to this category.

The second category consisted of homopolymer pairs [e.g. poly(dA)·poly(dT)] and poly(dI-dC)·poly(dI-dC), which reacted with Mitoxantrone similarly as with Ametantrone but only at very low D/P (below 0.02). Above this value an increase in light scattering becomes apparent, and the spectral changes suggested formation of secondary complexes (Figs. 4B and 5A). Although these secondary changes did not preclude the possibility of estimating the association constant K_I (because the calculation was based on extrapolation to r equal to zero and, therefore, the most significant were the titration points at low D/P), it could distort the values of binding site sizes as seen in Fig. 5B and Table 4.

The second type of binding sites for Mitoxantrone has been reported before by Foye *et al.* [18]. These authors observed such sites in the case of calf thymus DNA at very low ionic strength and explained it as an electrostatic interaction involving DNA phosphate groups and the amino side chains of the ligand. An ionic interaction of the drug with nucleic acids was also suggested in our earlier publication [5]. The electrostatic binding, however, cannot be explained in light of the presently observed differences in interaction between different DNAs and the drug at higher D/P ratios. Namely, according to the Manning–Record counter-ion condensation theory, affinities of ionic ligands to charged polymers are related to the charge densities of the latter [23, 24], which are similar for all DNAs in the B conformation. Minor conformational differences between synthetic DNAs cannot explain the dramatic differences in interaction of the drug with homopolymer-pairs vs alternating analogs [i.e. poly(dA)·poly(dT) vs poly(dA-dT)·poly(dA-dT) or poly(dG)·poly(dC) vs poly(dG-dC)·poly(dG-dC)] at higher D/P ratio, assuming electrostatic binding alone. Furthermore, it is difficult to envisage under the same assumption why poly(dI-dC)·poly(dI-dC) is much more reactive than poly(dG-dC)·poly(dG-dC), or why there is such differences between the drugs.

The possibility of electrostatic binding of the drugs outside the helix is clearly minor at the relatively high Na^+ concentration (0.15 M). According to the Manning–Record theory [23, 24], purely electrostatic ion–polymer interactions, albeit strong at low ionic strength, markedly decrease as the concentration of cations increases [25]. For another cationic intercalator, acridine orange, the K value of such interaction was estimated [11] to be approximately $10\ M^{-1}$ (in 0.1 NaCl), e.g. several orders of magnitude below those of the drugs presented in Table 4.

The experimental evidence that this type of interaction cannot play a significant role, at least in the case of Ametantrone, is the presence of a quasi-isosbestic point in the spectra of the DNA–drug mixtures at different D/P ratios (Fig. 3A). Because side chains of both drugs are identical (Fig. 1), it is safe to assume that this may be the case for Mitoxantrone, even if self-association precludes observation of quasi-isosbestic points for the latter (Fig. 4A). It should be stressed, however, that electrostatic interactions involving DNA phosphate groups and amino side chains of the ligand may accompany intercalation of the aromatic part of the ligand [5]. The presence of a quasi-isosbestic point indicates also that the spectral properties of the bound drug are independent of the binding density.

The increase in light scattering of DNAs titrated with Mitoxantrone [e.g. poly(dG)·poly(dC), Fig. 5A] suggested that condensation (collapse) of polymers may occur at higher D/P ratios. In earlier experiments, we have shown that this drug can condense nucleic acids very effectively [10]. Condensation of double-strand nucleic acids induced by some intercalators is preceded by their denaturation [9]. As a consequence of denaturation, the number of binding sites available for intercalation is expected to decrease. This phenomenon, therefore, may be responsible for the exceptionally large binding size calculated for poly(dI-dC)·poly(dI-dC) and other polymers for which the secondary binding process has been observed (Table 4). In addition, the spectra of the mixtures of poly(dA)·poly(dT) and Mitoxantrone at $D/P > 0.25$ (Fig. 4B) resemble spectra of the drug complexes with single-stranded nucleic acids and are not typical of the intercalative mode of binding [5].

The present data in conjunction with earlier observations [10] indicate that the intercalator-induced destabilization of the double-helix and subsequent condensation of polymers may play a dominant role in Mitoxantrone-nucleic acid interactions, at least in certain types of DNAs, and at higher D/P ratios. The observation may explain the apparent G-C specificity of the drug as reported by Foye *et al.* [8]. These authors studied inhibition of RNA polymerase by the drug and observed that the degree of inhibition was dependent upon the G-C content. The experiments were performed at low ionic strength in which the secondary type of binding sites was observed even for calf thymus DNA with moderate (43%) G-C base content. Base-specific inhibitory effects have been observed at high drug concentrations (100 μM, $D/P \simeq 0.3$). It has been reported that drug, at concentrations as low as 2–40 μM, can induce DNA condensation [10]. It is plausible therefore that at higher concentrations [8] part of the polymer has undergone condensation and becomes inaccessible to the enzyme. More extensive studies of this phenomenon indicate that indeed the pharmacological activities of Mitoxantrone and Ametantrone are correlated with their abilities to condense nucleic acids. These studies have been completed in our laboratory and are the subject of a separate paper.*

The summary results on the primary, intercalative mode of binding of the studied ligands to DNA are more clear and can be formulated as follows:

(1) No clear DNA base-specificity, for both drugs, as measured by the value of the intrinsic association constant (K_I), was detected (Table 4). This conclusion, based on more accurate studies, is in general agreement with the results of the previous investigations [5, 7].

(2) Intrinsic association constants of Mitoxantrone and Ametantrone are of a similar magnitude with somewhat higher values for the latter. Thus, no correlation between the intercalative mode of ligand binding to DNA and its pharmacological activity is apparent.

* J. Kapuscinski and Z. Darzynkiewicz, manuscript in preparation.

Note added in proof: Recently published studies by J. W. Lawn *et al.* [*Biochemistry* **24**, 4028 (1985)] indicate that in 0.5 N NaCl Mitoxantrone has higher affinity to calf thymus DNA than Ametantrone. These data, however, cannot be directly compared with our present results. Namely, in addition to working at higher ionic strength as compared to our studies and also uncertainty in the "*n*" estimate for Ametantrone, the authors used the reverse titration method (drug titrated with DNA) in which, from the beginning of the titration a high drug/DNA ratio exists, i.e. the situation as described in Fig. 5. Under these conditions an immediate condensation of the most sensitive section of DNA may occur, affecting the intercalation.

Acknowledgements—We are grateful to Dr. Myron R. Melamed for his constant support and encouragement, to Drs. Frank Traganos and Marek Kimmel for helpful discussion, and to Mrs. Sally Carter and Mrs. Patricia Higgins for their assistance in the preparation of the manuscript. This work was supported by U.S. Public Health Service Grants CA 28704 and CA 23296.

REFERENCES

1. R. K-Y. Zee-Cheng and C. C. Cheng, *J. med Chem.* **21**, 291 (1978).
2. F. Traganos, *Pharmac. Ther.* **22**, 199 (1983).
3. J. R. Brown, in *Molecular Aspects of Anti-Cancer Drug Action* (Eds. S. Neidle and M. J. Waring), p. 57. The Contributors, London (1983).
4. F. E. Durr, R. E. Wallace and R. V. Citarella, *Cancer Treat. Rev.* **10** (Suppl. B), 3 (1983).
5. J. Kapuscinski, Z. Darzynkiewcz, F. Traganos and M. R. Melamed, *Biochem. Pharmac.* **30**, 231 (1981).
6. A. R. Safa, N. Chegini and M. T. Tseng, *J. cell. Biochem.* **22**, 111 (1983).
7. J. Roboz, C. L. Richardson and J. F. Holland, *Life Sci.* **31**, 25 (1982).
8. W. O. Foye, O. Vajragupta and S. K. Sengupta, *J. pharm. Sci.* **71**, 253 (1982).
9. J. Kapuscinski and Z. Darzynkiewicz, *J. biomolec. Struct. Dynamics* **1**, 1485 (1984).
10. J. Kapuscinski and Z. Darzynkiewicz, *Proc. natn. Acad. Sci. U.S.A* **81**, 7368 (1984).
11. J. Kapuscinski, Z. Darzynkiewicz and M. R. Melamed, *Biochem. Pharmac.* **32**, 3679 (1983).
12. J-B. LePecq and C. Paoletti, *J. molec. Biol.* **27**, 87 (1967).
13. D. Elson, P. Spitnik-Elson, S. Avital and R. Abramowitz, *Nucleic Acids Res.* **7**, 465 (1979).
14. V. von Tscharner and G. Schwarz, *Biophys. Struct. Mechanism* **5**, 75 (1979).
15. J. D. McGhee and P. H. von Hippel, *J. molec. Biol.* **86**, 469 (1974).
16. W. D. Wilson and I. G. Lopp, *Biopolymers* **18**, 3025 (1979).
17. H. Porumb, *Prog. Biophys. molec. Biol.* **34**, 175 (1978).
18. R. K. Johnson, R. K-Y. Zee-Cheng, W. W. Lee, E. M. Acton, D. W. Henry and C. C. Cheng, *Cancer Treat. Rep.* **63**, 425 (1979).
19. J. W. Lawn, C. C. Hanstock, R. D. Bradley and D. G. Scraba, *Molec. Pharmac.* **25**, 178 (1984).
20. D. M. Crothers, *Biopolymers* **6**, 575 (1968).
21. W. D. Wilson and R. L. Jones, in *Intercalation Chemistry* (Eds. M. S. Whittingham and A. J. Jacobson), p. 445. Academic Press, New York (1982).
22. L. S. Lerman, *J. molec. Biol.* **3**, 18 (1961).
23. G. S. Manning, *Q. Rev. Biophys.* **11**, 179 (1978).
24. M. T. Record, Jr., T. M. Lohman and P. de Haseth, *J. molec. Biol.* **107**, 145 (1976).
25. R. L. Jones, A. C. Lanier, R. A. Keel and W. D. Wilson, *Nucleic Acids Res.* **8**, 1613 (1980).